GABA$_B$ Receptor Activation Modulates GABA$_A$ Receptor–Mediated Inhibition in Chicken Nucleus Magnocellularis Neurons

Yong Lu, R. Michael Burger, and Edwin W Rubel
Virginia Merrill Bloedel Hearing Research Center, Department of Otolaryngology-Head and Neck Surgery,
University of Washington, Seattle, Washington

Lu, Yong, R. Michael Burger, and Edwin W Rubel. GABA$_B$ receptor activation modulates GABA$_A$ receptor–mediated inhibition in chicken nucleus magnocellularis neurons. *J Neurophysiol* 93: 1429–1438, 2005; doi:10.1152/jn.00786.2004. Neurons of nucleus magnocellularis (NM), a division of avian cochlear nucleus that performs precise temporal encoding, receive glutamatergic excitatory input solely from the eighth nerve and GABAergic inhibitory input primarily from the ipsilateral superior olivary nucleus. GABA activates both ligand-gated Cl$^-$ channels [GABA$_A$ receptors (GABA$_A$Rs)] and G protein–coupled receptors (GABA$_B$ receptors). The net effect of GABA$_A$R-mediated input to NM is inhibitory, although depolarizing. Several studies have shown that this shunting, inhibitory GABAergic input can evoke action potentials in postsynaptic NM neurons, which could interfere with their temporal encoding. While this GABA-mediated firing is limited by a low-voltage–activated K$^+$ conductance, we have found evidence for a second mechanism. We investigated modulation of GABA$_A$R-mediated responses by GABA$_B$Rs using whole cell recording techniques. Bath-applied baclofen, a GABA$_B$R agonist, produced dose-dependent suppression of evoked inhibitory postsynaptic currents (eIPSCs). This suppression was blocked by CGP52432, a potent and selective GABA$_B$R antagonist. Baclofen reduced the frequency but not the amplitude of miniature IPSCs (mIPSCs) and did not affect postsynaptic currents elicited by puff application of a specific GABA$_A$R agonist muscimol, suggesting a presynaptic mechanism for the GABA$_B$R-mediated modulation. Firing of NM neurons by synaptic stimulation of GABAergic inputs to NM was eliminated by baclofen. However, endogenous GABA$_B$R activity in the presynaptic inhibitory terminals was not observed. We propose that presynaptic GABA$_B$Rs function as autoreceptors, regulating synaptic strength of GABA$_A$R-mediated inhibition, and prevent NM neurons from generating firing during activation of the inhibitory inputs.

INTRODUCTION

GABA$_B$ receptors (GABA$_B$Rs) expressed on presynaptic terminals function as either autoreceptors modulating GABA release or heteroreceptors modulating release of other transmitters (reviewed in Calver et al. 2002; Misgeld et al. 1995). Chicken nucleus magnocellularis (NM) neurons receive excitatory input from the eighth nerve and GABAergic inhibitory input primarily from the ipsilateral superior olivary nucleus (SON) (Burger et al. 2005; Lachica et al. 1994; Parks and Rubel 1978; Yang et al. 1999). GABA$_B$Rs are expressed postsynaptically in NM neurons and presynaptically on terminals of both excitatory and inhibitory inputs (Pfeiffer et al. 2003). GABA$_B$R-mediated modulation of the excitatory in-

puts to NM has been described; activation of presynaptic GABA$_B$Rs reduces the excitatory postsynaptic currents (EPSCs) to NM (Otis and Trussell 1996) and enhances the synaptic efficacy of the excitatory inputs during high-frequency firing (Brenowitz and Trussell 2001; Brenowitz et al. 1998). The function of the GABA$_B$Rs on the inhibitory terminals impinging on NM neurons remains unknown.

Functionally similar to bushy cells in mammalian cochlear nucleus, NM neurons respond to the excitatory inputs from the auditory nerve in a phase-locked manner and perform precise temporal encoding (reviewed in Oertel 1999; Trussell 1999). This temporal precision is critical in that NM neurons provide the sole excitatory input to nucleus laminaris (NL) neurons, the first nucleus to encode interaural time differences (ITDs) (Parks and Rubel 1975; Rubel and Parks 1975). NL neurons compute ITDs with accuracy on the order of tens of microseconds (Pena et al. 1996). The phase-locking fidelity of NM neurons is enhanced, in part, by activation of the GABAergic inputs from the SON (Monsivais et al. 2000). An unusual feature of the GABAergic input to NM is that it is depolarizing, due to a high intracellular Cl$^-$ concentration in NM neurons that persists into maturity (Hyson et al. 1995; Lachica et al. 1994; Lu and Trussell 2001; Monsivais and Rubel 2001). Although depolarizing, the GABAergic inputs produce a potent net inhibitory effect by reducing the input resistance and activating a K$^+$ conductance while inactivating Na$^+$ channels in NM neurons (Monsivais and Rubel 2001). However, such depolarizing inhibitory inputs to NM may be problematic. The reversal potential of GABA$_A$R-mediated responses in NM neurons is 10–20 mV more positive than the action potential (AP) threshold of NM neurons (Lu and Trussell 2001; Monsivais and Rubel 2001). Thus synaptic activation of the GABAergic inputs occasionally evokes APs (Lu and Trussell 2001). Since these inputs are unlikely to phase-lock to the auditory inputs (Lachica et al. 1994; Yang et al. 1999), such spurious AP generation may interfere with temporal encoding of acoustic information by NM neurons.

One mechanism reducing the probability of GABA-induced AP generation by NM neurons is the low-voltage–activated (LVA) K$^+$ conductance, which is activated at slightly more positive membrane potentials than the resting membrane potential (Monsivais and Rubel 2001). Depolarization-induced LVA K$^+$ conductance can suppress firing due to activation of GABAergic inputs. When the LVA K$^+$ channels are blocked, firing in response to synaptic stimulation of the inhibitory

inputs is greatly facilitated (Monsivais and Rubel 2001). However, Lu and Trussell (2001) have indicated that LVA K⁺ activation does not block all GABA-evoked AP generation. Here we propose a second mechanism that involves $GABA_BRs$ located on the inhibitory presynaptic terminals. We show that presynaptic $GABA_BRs$ limit GABA release. We also show that this mechanism is sufficient to suppress the GABA-evoked discharges in NM. Some data included in this study have been presented in abstract form (Lu et al. 2004).

METHODS

Slice preparation and in vitro whole cell recordings

Brain stem slices (200–250 μm thickness) were prepared from E18–E21 chicken embryos, as described previously (Monsivais et al. 2000; Reyes et al. 1994). For recording, slices were transferred to a 0.5-ml chamber mounted on a Zeiss Axioskop FS (Zeiss) with a 40× water-immersion objective and infrared, differential interference contrast (DIC) optics. The chamber was continuously superfused with artificial cerebrospinal fluid (ACSF; 2–3 ml/min) containing (in mM) 130 NaCl, 26 NaH_2CO_3, 3 KCl, 3 $CaCl_2$, 1 $MgCl_2$, 1.25 NaH_2PO_4, and 10 dextrose and was constantly gassed with 95% O_2-5% CO_2 (pH 7.4). Voltage-clamp experiments were performed with an Axopatch 200B amplifier, whereas current-clamp experiments were performed with an Axoclamp 2B amplifier (Axon Instruments, Union City, CA). Recordings were performed at 34–36°C.

Patch pipettes were drawn to 1- to 2-μm tip diameter and had resistances between 3 and 7 MΩ. Pipettes were filled with a solution containing (in mM) 105 K-gluconate, 35 KCl, 5 EGTA, 10 HEPES, 1 $MgCl_2$, 4 ATP-Mg, and 0.3 GTP-Na, pH 7.2 adjusted with KOH, and osmolarity was between 280 and 290 mOsm. For some recordings ($n = 4$ cells), a Cs-based internal was used, containing (in mM) 105 Cs-methanesulfonate, 35 CsCl, 5 EGTA, 10 HEPES, 1 $MgCl_2$, 4 ATP-Mg, 0.3 GTP-Na, and 5 QX-314, pH 7.2 adjusted with CsOH, and osmolarity was between 280 and 290 mOsm. The Cl^- concentration (37 mM) in both internal solutions approximated the physiological Cl^- concentration in NM neurons (Monsivais and Rubel 2001). The liquid junction potential was 10 mV for both the K- and Cs-based internal solutions, respectively, and data were corrected accordingly. Data were low-pass filtered at 3 or 5 kHz and digitized with an ITC-16 (Instrutech, Great Neck, NY) at 20 kHz for both on- and off-line analyses. All recording protocols were written and run using the acquisition and analysis software Axograph, version 4.5 (Axon Instruments). Means and SD are reported in the text, and means and SE are shown in figures.

In each voltage-clamp recording, series resistance was compensated by 80–90%, and cells were clamped at a membrane potential of −70 mV. Before each synaptic stimulation protocol was applied, a 5 mV hyperpolarizing command (5 ms duration) was given to monitor series resistance and input resistance during the experiment. When measuring the reversal potentials for either evoked or miniature inhibitory postsynaptic currents (eIPSCs or mIPSCs), we changed the membrane potentials from −80 to 0 mV, in steps of 10 or 20 mV. In all experiments, antagonists for ionotropic glutamate receptors (50 μM DNQX and 100 μM AP-5) were included in ACSF, and 1 μM TTX was added when recording mIPSCs. Events of mIPSCs were detected by a threshold method from chart recordings.

All chemicals and drugs were obtained from Sigma (St. Louis, MO) except CGP52432 and CGP54626, which were obtained from Tocris (Ballwin, MO). Drugs were bath-applied unless otherwise indicated.

Synaptic stimulation and puff application

Extracellular stimulation was performed using concentric bipolar electrodes (Frederick Haer, Bowdoinham, ME) with a tip diameter of 200 μm. The electrode was placed in the fiber tract dorsal to NM. Square electric pulses of 100- to 300-μs duration were delivered through a stimulus isolator 1850A and an interval generator 1830 (W-P Instruments, New Haven, CT). The stimulus was either a single-pulse or a train of pulses at an intensity of 5–90 V. Optimal stimulation parameters were selected for each cell to give maximal amplitude of postsynaptic currents or potentials and lowest failure rate.

Puff application of muscimol, a specific $GABA_AR$ agonist, was done by using a multi-channel picospritzer (General Valve, Fairfield, NJ). Muscimol (500 μM) was prepared in ACSF containing 50 μM DNQX and 100 μM AP-5. Puff electrodes were prepared using the same pulling methods as producing recording electrodes except that puff electrodes have larger tip diameter (2–5 μm). The puff electrode was placed to the side and above the cell studied with a distance between the cell and the electrode tip of 50–100 μm. Positive pressure (5–10 psi and duration of 10–50 ms) was used to eject the solution (ACSF) containing muscimol.

Data analysis

Peak amplitudes of averaged eIPSCs were measured after normalizing the baseline several milliseconds before the stimulation artifacts. Percent inhibition is defined as 100 × (mean eIPSC amplitude under control condition −mean eIPSC amplitude under drug)/mean eIPSC amplitude under control condition. Failures of evoked currents can be readily detected by visual inspection, and failure rate is defined as 100 × (number of failures)/total number of stimulation pulses. Statistics were performed using Excel (Microsoft, Redmond, WA) and Statview (Abacus Concepts, Berkeley, CA), and graphs were made in Igor (Wavemetrics, Lake Oswego, OR).

RESULTS

$GABA_AR$-mediated responses in NM neurons

eIPSCs were recorded in the presence of ionotropic glutamate receptor (iGluR) blockers (50 μM DNQX and 100 μM AP-5). The amplitude of eIPSCs in response to repeated single-pulse synaptic stimulation varied substantially (Fig. 1A), similar to what has been previously reported (Lu and Trussell 2000). Synaptic failures were readily detected by visual inspection. Both eIPSCs and mIPSCs reversed at a potential close to the predicted reversal potential (−35 mV) calculated from Nernst equation (data not shown). Furthermore, both the eIPSCs and the mIPSCs were completely eliminated by 20 μM bicuculline (data not shown), a $GABA_AR$ antagonist, confirming that the recorded eIPSCs and mIPSCs were mediated by $GABA_ARs$.

eIPSCs in response to train stimulation

Train stimulation (10 Hz, 5 pulses) was used as our standard stimulation protocol to access modulation of $GABA_BRs$ on $GABA_AR$-mediated responses. Under voltage-clamp configuration, activation of GABAergic inputs to NM by the train stimulation produced individually distinguishable eIPSCs that showed a mix of facilitation and depression, and the pattern was consistent both among individual neurons and across the population (Fig. 1, A–C), similar to previous reports (Lu and Trussell 2000). Pooled data ($n = 23$ cells) shown in Fig. 1C revealed the same pattern of facilitation and depression as the sample neuron, independent of occurrence of failures. When failures were included, the mean amplitudes of the eIPSCs in response to the first through the fifth pulse were −188 ± 168,
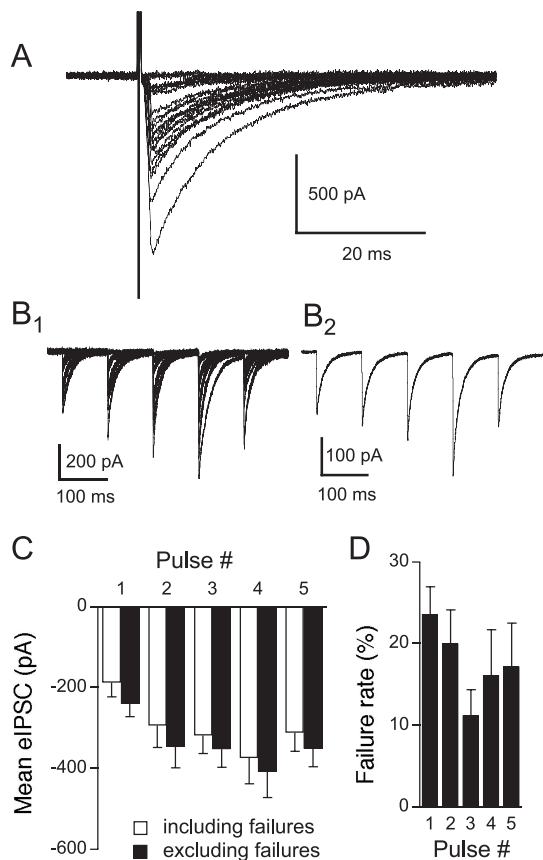
FIG. 1. Basic properties of GABAergic transmission in nucleus magnocellularis (NM): evoked inhibitory postsynaptic currents (eIPSCs) in response to single-pulse and train stimulation (10 Hz, 5 pulses). *A*: eIPSCs to single-pulse stimulation (24 repetitions). Amplitude of eIPSCs varies widely, and some failures are present. Stimulation artifacts are truncated for clarity. B_1: representative individual eIPSCs to train stimulation (12 repetitions). B_2: average of the traces shown in B_1 shows a mix of facilitation and depression. *C*: pooled data (*n* = 23 cells, obtained from cells under control conditions presented in Figs. 2–4, and 4 other cells whose data not shown) show same facilitation and depression pattern of eIPSCs to train stimulation, independent of occurrence of failures. *D*: failure rates (defined as percentage of pulses resulting in failures over total number of pulses) across stimulation pulses (*n* = 23 cells). Failure rate to the 1st pulse (24%) is approximately equal to failure rate of eIPSCs in response to single-pulse stimulation (23%). Cells were held at a membrane potential of −70 mV for voltage-clamp experiments. In this and subsequent figures, we show means ± SE. Note that means and SD are reported in the text.

−294 ± 262, −319 ± 213, −374 ± 306, and −311 ± 219 pA, respectively (Fig. 1*C,* open bars). Note that means and SD are reported in the text, and means and SE are showed in figures. When failures were excluded, the mean amplitudes of the eIPSCs in response to the first through the fifth pulse averaged 43 pA higher but showed the same pattern (Fig. 1*C,* filled bars). Failure rate varies from cell to cell as well as among different groups of cells. Figure 1*D* shows the failure rates in response to different pulses of the train stimulation. The data were obtained from all cells from which eIPSCs were recorded. The total failure rate to all pulses averaged 18 ± 17% (*n* = 23 cells), with a broad range (0–55%) among individual cells. Therefore failure rates in subsequent figures representing subpopulations of this total failure rate reflect this range with mean control failure rates ranging between 6 and 28%.

To verify that the failures in our eIPSC recordings were failures of transmitter release as opposed to propagation of the

stimulated axons, we studied the relationship between extracellular calcium concentration ($[Ca^{2+}]_o$) and the amplitude and failure rate of eIPSCs. This paradigm is often used to indirectly distinguish axonal conduction versus release failures (Allen and Stevens 1994; Canepari and Cherubini 1998; Debanne et al. 1996; Jiang et al. 2000). $[Ca^{2+}]_o$ and $[Mg^{2+}]_o$ were varied, but the total amount of divalent ions was unchanged to keep the axonal excitability the same. Figure 2*A* shows four averaged traces obtained under standard solution (control condition, 3 mM $[Ca^{2+}]_o$ and 1 mM $[Mg^{2+}]_o$) and three other conditions (1 mM $[Ca^{2+}]_o$ and 3 mM $[Mg^{2+}]_o$, 2 mM $[Ca^{2+}]_o$ and 2 mM $[Mg^{2+}]_o$, and 3.9 mM $[Ca^{2+}]_o$ and 0.1 mM $[Mg^{2+}]_o$). At $[Ca^{2+}]_o$ of 1 or 2 mM, the eIPSCs were smaller than the ones obtained under standard solution, and at $[Ca^{2+}]_o$ of 3.9 mM, the responses were larger, independent of occurrence of failures. For statistical analysis, the average of the peak values of the five eIPSCs under each condition was treated as one data-point for each cell. We calculated the ratio of mean eIPSC of the experimental conditions ($[Ca^{2+}]_o$ = 1, 2, and 3.9 mM for *n* = 6, 3, and 5 cells, respectively) to that of our standard condition ($[Ca^{2+}]_o$ = 3 mM). These ratios are shown in Fig. 2*B* with and without inclusion of failures. ANOVA showed a highly significant trend in both analyses ($P < 0.001$).

The failure rate also changed with $[Ca^{2+}]_o$ in a predictable way: 1 mM $[Ca^{2+}]_o$ solution gave rise to the highest failure rate (46 ± 28%, *n* = 6 cells), and failure rate declined with increased $[Ca^{2+}]_o$, being 22 ± 21 (*n* = 3 cells), 6 ± 10 (*n* = 6 cells), and 10 ± 12% (*n* = 5 cells) at 2, 3, and 3.9 mM $[Ca^{2+}]_o$, respectively (Fig. 2*C*). Although axonal failures, if any, cannot be ruled out completely, these results strongly suggested that the failures we observed are largely failures of Ca^{2+}-dependent transmitter release.
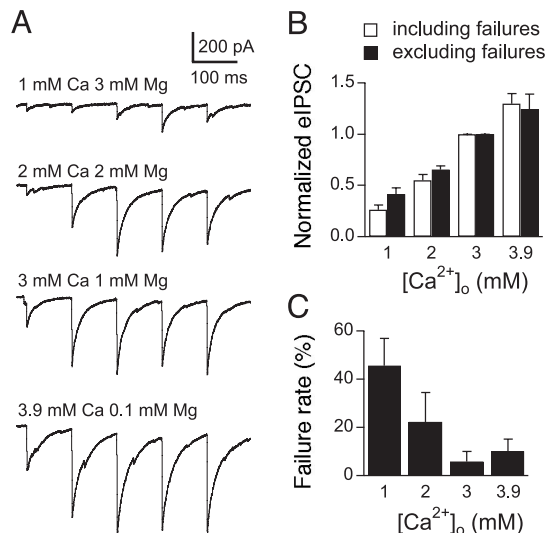

FIG. 2. Synaptic failures are largely due to failures of transmitter release, not failures of axonal stimulation. *A*: average eIPSCs recorded at different $[Ca^{2+}]_o$ (1, 2, 3, and 3.9 mM), with equivalent total divalent ions concentration ($[Mg^{2+}]_o$ at 3, 2, 1, and 0.1 mM, respectively). Note systematic change in amplitude of eIPSCs as a function of $[Ca^{2+}]_o$. *B*: peak amplitude of average eIPSCs, normalized to amplitude of eIPSCs obtained in standard solution (3 mM $[Ca^{2+}]_o$ and 1 mM $[Mg^{2+}]_o$), is plotted against $[Ca^{2+}]_o$, showing that release of GABA at NM is $[Ca^{2+}]_o$-dependent. *C*: failure rate decreases correspondingly with increasing $[Ca^{2+}]_o$.
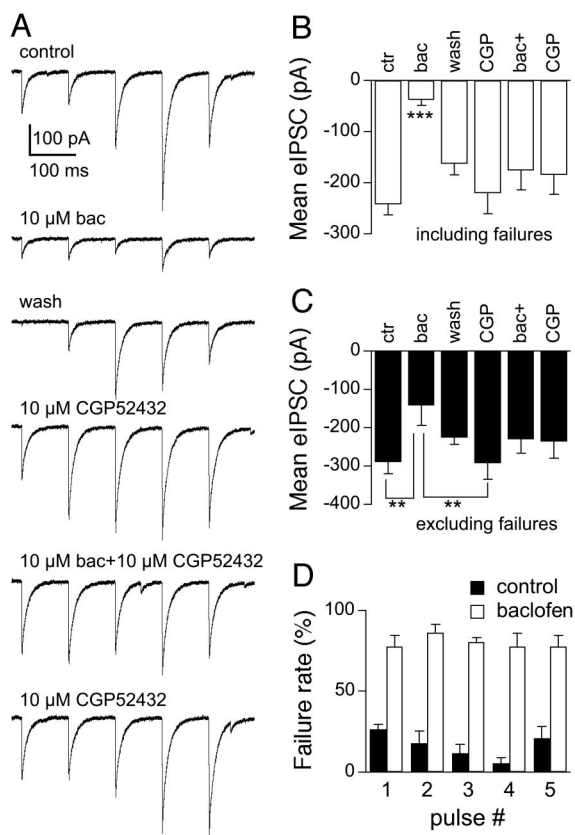
FIG. 3. GABA$_B$ receptor (GABA$_B$R) activation inhibits eIPSCs in NM neurons. *A*: average eIPSCs obtained under conditions of control, GABA$_B$R agonist (10 μM baclofen), washout of the 1st baclofen application, GABA$_B$R antagonist (10 μM CGP52432), baclofen (10 μM) plus CGP52432 (10 μM), and washout of the 2nd baclofen application (in 10 μM CGP52432). The 2nd baclofen application was done in the presence of CGP52432, which was applied for about 2 min prior to baclofen. *B*: when failures are included, baclofen (10 μM) inhibits eIPSCs significantly (*n* = 6 cells, ANOVA, *P* < 0.001), and significant difference is detected between the 1st baclofen application and any other group. In the presence of 10 μM CGP52432, the inhibitory effect of baclofen on eIPSCs is blocked (bac+: 10 μM baclofen plus 10 μM CGP52432). *C*: when failures are excluded, reduction of eIPSCs by the 1st baclofen application is decreased (ANOVA, *P* > 0.05; but Fisher's test shows significant difference between the 1st baclofen application and control or CGP52432, *P* < 0.01). *D*: baclofen produces high and stable failure rates across the train stimulation.

GABA$_B$R activation inhibits eIPSCs

We examined the effects of GABA$_B$R agonist and antagonist on GABA$_A$R-mediated responses in NM neurons by recording eIPSCs with the standard 10-Hz 5-pulse train stimulation once every 10 s for 15–20 min during which specific GABA$_B$R agonist baclofen (10 μM) and antagonist CGP52432 (10 μM) were bath-applied. Figure 3*A* shows six averaged traces from a representative NM neuron obtained under the following conditions: control, 10 μM baclofen, washout of baclofen, 10 μM CGP52432, baclofen plus CGP52432, and 10 μM CGP52432 (washout of the 2nd baclofen application). The first baclofen application reduced eIPSCs substantially and caused a high failure rate (not shown in the 2nd trace in Fig. 3*A* because the trace is an averaged response from 6 raw traces). Figure 3, *B* and *C*, provides averaged data from six NM neurons including and excluding failures, respectively. The same trend is seen in each analysis. Baclofen (10 μM) reliably inhibits the eIPSC,

and this effect is blocked by the GABA$_B$R antagonist CGP52432 (10 μM). Comparison of Fig. 3, *B* and *C,* indicates that the effects of baclofen on eIPSCs are due to both an increase of failure rate and a decrease in the size of evoked responses. Input resistance, monitored by current responses to a 5-mV hyperpolarizing command (duration of 5 ms) that precedes each stimulation protocol, remained unchanged during the experiment (data not shown).

The kinetics of eIPSCs under all six conditions was stable (data not shown), suggesting that GABA$_B$R activation inhibits eIPSCs without affecting GABA$_A$R channel properties such as time course of activation and deactivation. Figure 3*D* shows that baclofen application produces a high and stable failure rate (averaging 80%) across the five pulses, whereas under control condition, the failure rate averaged 16% (*P* < 0.001).

Independent of occurrence of failures, the suppressive effect of baclofen on the amplitude of eIPSCs was dose-dependent. When failures were included, at concentrations of 0.1, 1, 10, and 100 μM, baclofen produced average reductions of 31 ± 19 (*n* = 3 cells), 52 ± 11 (*n* = 6 cells), 83 ± 10 (*n* = 6 cells), and 93 ± 5% (*n* = 4 cells), respectively (Fig. 4*A,* open bars; ANOVA, *P* < 0.001). When failures were excluded, the percent reductions were 27 ± 11, 31 ± 19, 66 ± 26, and 91 ± 8%, respectively (Fig. 4*A,* filled bars; ANOVA, *P* < 0.001). The IC$_{50}$ of baclofen was estimated to be at about 1 μM in that baclofen (1 μM) produced ~50% inhibition of the eIPSCs. Baclofen (100 μM) induced an almost complete block of the GABAergic transmission, suggesting that GABA$_B$R activation has the capability of shutting down nearly completely the inhibitory inputs at NM (Fig. 4*C*). The effect of baclofen on the total failure rate also showed dose-dependence; the failure rate under control condition was 28 ± 19% (*n* = 7 cells) and
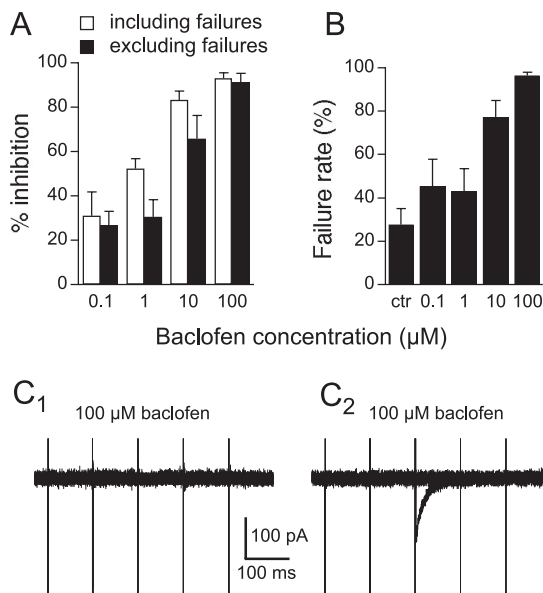

FIG. 4. Effects of baclofen on amplitude of GABA$_A$R-mediated eIPSCs and failure rate are dose-dependent. *A*: percent inhibition of eIPSCs increases as a function of baclofen concentration (*n* = 3, 6, 6, and 4 cells for 0.1, 1, 10, and 100 μM, respectively) independent of occurrence of failures. *B*: average failure rate increases with increasing baclofen concentration. *C$_1$*: 5 superimposed original current traces during baclofen (100 μM) application in 1 NM neuron show that baclofen completely shut down GABAergic transmission. In another NM neuron, 1 eIPSC was observed (*C$_2$*).
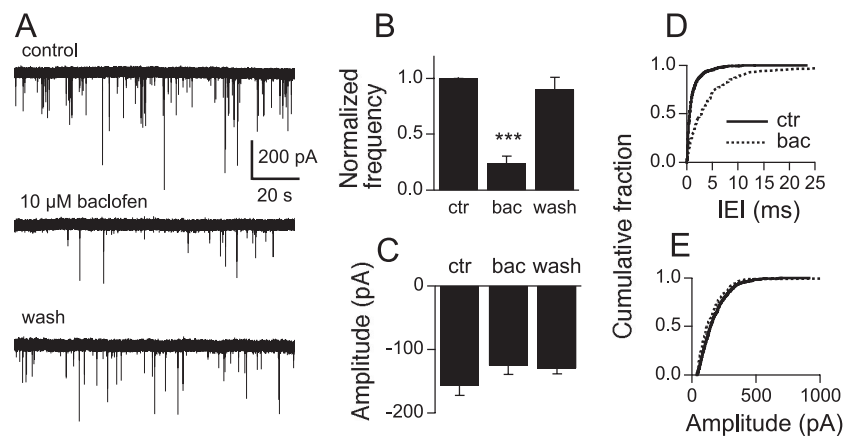
FIG. 5. Effects of baclofen on miniature IPSCs (mIPSCs) of NM neurons. *A*: representative example in which mIPSCs were recorded before, during, and after 10 μM baclofen application. *B*: GABA$_B$R activation by baclofen significantly reduces frequency of mIPSCs (ANOVA, $P <$ 0.001, $n = 10$ cells). *C*: baclofen does not have significant effects on the mean amplitude of mIPSCs (ANOVA, $P >$ 0.05). *D* and *E*: cumulative distribution of interevent interval (IEI) and amplitude of mIPSCs (1,037 and 197 events for control and baclofen, respectively; for clarity, 6 (3.2%) events with IEI >25 s during baclofen application were not shown).

increased to 96 $\pm$ 3% at 100 μM baclofen application (Fig. 4*B*; ANOVA, $P <$ 0.001).

GABA$_B$R activation modulates GABA$_A$R-mediated responses via a presynaptic mechanism

We used two approaches to examine whether the GABA$_B$R-mediated modulation of inhibitory transmission in NM is due to a presynaptic, postsynaptic, or dual mechanism. The first approach evaluated the effect of baclofen on mIPSCs recorded in the presence of TTX (1 μM); modulation of the frequency but not the amplitude of mIPSCs would imply a presynaptic mechanism (Chen and van den Pol 1998; Jarolimek and Misgeld 1997; Kabashima et al. 1997). As shown in Fig. 5, this is indeed what we observed. Figure 5*A* shows representative results from one NM neuron, and Fig. 5, *B* and *C*, shows group data. Baclofen (10 μM) reliably reduced the frequency of mIPSCs to 24 $\pm$ 21% of the control (Fig. 5*B*; ANOVA, $P <$ 0.001, $n = 10$ cells), but did not significantly influence the amplitude of mIPSCs; the amplitude of mIPSCs was $-157 \pm$ 47, $-125 \pm$ 45, and $-130 \pm$ 28 pA for control, baclofen, and wash condition, respectively (Fig. 5*C*; ANOVA, $P >$ 0.05, $n =$ 10 cells). In the presence of GABA$_B$R antagonist CGP52432 (10 μM), the inhibitory effect of baclofen (10 μM) on the frequency of mIPSCs was blocked ($n = 3$ cells, data not shown). The normalized frequency of mIPSCs under this condition was 93% of control condition ($P >$ 0.05), confirming that the modulation is mediated by GABA$_B$Rs. Figure 5, *D* and *E*, shows that, although there were fewer mIPSCs during baclofen application, the distribution of mIPSC amplitudes was similar to that under control conditions.

The second approach was to evaluate the effect of baclofen on the postsynaptic responses elicited by local application of the specific GABA$_A$R agonist muscimol (Fig. 6). Pressure ejection of muscimol (500 μM) generated a large, slow inward current in the presence of antagonists for iGluRs at the membrane potential of –70 mV (Fig. 6*A, inset*). The current was sensitive to bicuculline (80 μM), which blocked 91.2 $\pm$ 6.2% of the total current ($n = 2$ cells, data not shown). In the example shown in Fig. 6*A*, the current showed a slight rundown over time but did not change during 100 μM baclofen application. Figure 6*B* shows the mean current ($n = 4$ cells) in response to 500 μM muscimol before and during bath application of 100 μM baclofen. Paired *t*-test on pooled data

detected no significant difference in the mean current amplitudes ($P >$ 0.05). These results suggest that GABA$_B$R activation inhibits the GABA$_A$R-mediated responses via a presynaptic, not a postsynaptic, mechanism. This conclusion also is supported by the observation noted above that baclofen increased the failure rate of eIPSCs in a dose-dependent manner (Fig. 4*B*).

Postsynaptic GABA$_B$Rs can modulate a variety of ion channels especially K$^+$ channels in the CNS (reviewed in Calver et al. 2002; Misgeld et al. 1995). To further test whether postsynaptic GABA$_B$Rs are involved in the modulation of the inhibitory transmission at NM, we replaced K$^+$ with Cs$^+$ and included QX-314 (5 mM) in the recording pipettes to block postsynaptic K$^+$ and Na$^+$ channels and repeated the experiments testing the effects of baclofen on eIPSCs. Baclofen at its saturating concentration (100 μM) produced almost complete inhibition (91 $\pm$ 5%, $n = 4$ cells) of eIPSCs recorded using the Cs-based internal solution, similar to the percent inhibition induced by 100 μM baclofen when using the K-based internal solution (93 $\pm$ 5%, Fig. 4*A*, $n = 4$ cells), indicating that the effect of postsynaptic GABA$_B$Rs on postsynaptic K$^+$ channels,
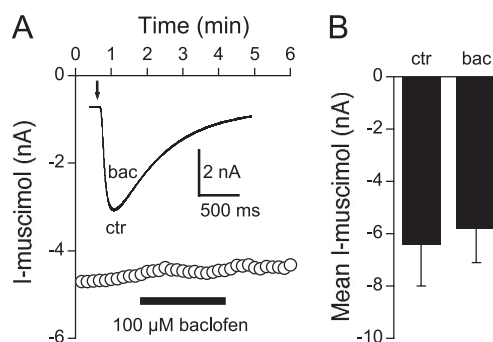

FIG. 6. Baclofen (100 μM) does not reliably influence postsynaptic ionotropic GABA response. *A*: puff application of muscimol (500 μM), a specific GABA$_A$R agonist, gives rise to a large, slow, and bicuculline-sensitive inward current (*inset*: arrow indicates puff application). As shown in the graph, baclofen does not significantly affect peak current. *Inset*: 2 averaged traces are plotted, 1 under control condition (last 6 traces prior to baclofen) and 1 after 1 min of baclofen application (last 6 traces during baclofen). The 2 traces nearly completely overlap, indicating that baclofen does not influence kinetics of the response to muscimol. *B*: pooled data show no significant difference in peak amplitude of current between control and baclofen conditions ($n = 4$ cells, paired *t*-test, $P >$ 0.05).
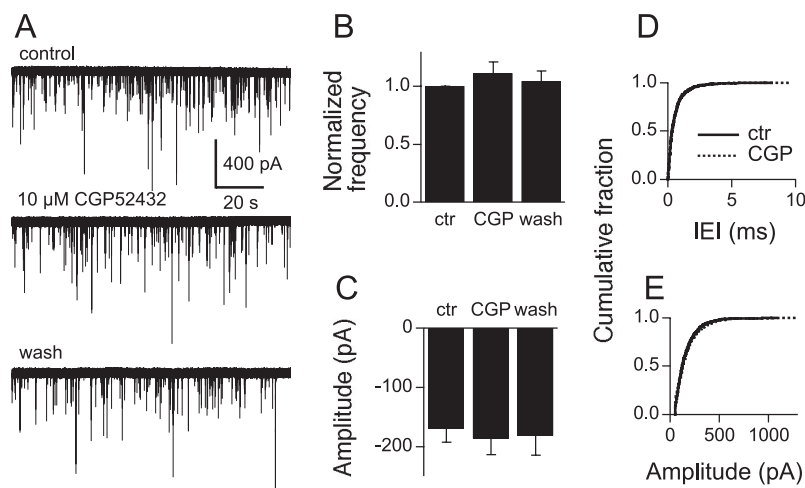
FIG. 7. Endogenous GABA$_B$R activation in inhibitory presynaptic terminals of NM neurons is lacking in vitro. *A*: example in which mIPSCs were recorded under control, GABA$_B$R antagonist CGP52432 (10 μM), and washout conditions. *B* and *C*: CGP52432 (10 μM) did not reliably increase frequency or amplitude of mIPSCs (ANOVA, $P > 0.05$). *D* and *E*: cumulative distributions of IEI and amplitude of mIPSCs are nearly identical under the 2 conditions (1,346 and 1487 events for control and CGP52432, respectively).

if any, is not involved in the modulation of the inhibitory transmission at NM.

Effect of GABA$_B$R antagonist CGP52432 on mIPSCs

To determine whether there is endogenous presynaptic GABA$_B$R activity at the inhibitory terminals in NM in vitro, we examined the effects of bath-applied GABA$_B$R antagonist CGP52432 (10 μM) on mIPSCs of NM neurons. The frequency of mIPSCs (normalized to control) was 1.13 ± 0.26 and 0.86 ± 0.23 for CGP52432 and wash condition, respectively (ANOVA, $P > 0.05$; $n = 7$ cells). The amplitude of mIPSCs was -169 ± 62, -186 ± 72, and -181 ± 89 pA for control, CGP52432, and wash condition, respectively (ANOVA, $P > 0.05$; $n = 7$ cells). The distributions of the interevent intervals and the amplitude of the mIPSCs during CGP52432 application were nearly identical to those under control conditions (Fig. 7, *D* and *E*).

Effect of GABA$_B$R agonist and antagonist on GABA-evoked firing

We used the current-clamp configuration to study APs generated by stimulation of GABAergic axons. In the presence of antagonists for iGluRs, we observed GABA$_A$R-mediated APs on the top of evoked inhibitory postsynaptic potentials (eIPSPs) in 13 of 41 (32%) NM neurons (37 mM Cl$^-$ in recording pipettes) when single-pulse stimulation of the GABAergic inputs was applied. The results of GABA$_B$R agonist and antagonists on APs in these cells are shown in Fig. 8. Responses to single-pulse stimulation were tested for all neurons so that our data could be compared with previous studies (see DISCUSSION). Cells that showed GABA-induced APs to single-pulse stimulation also fired spikes in response to train stimulation (10 or 5 Hz; 5 pulses). In contrast, cells that did not fire spikes to single-pulse stimulation also failed to fire spikes to train stimulation (5–200 Hz; 5–20 pulses). Bicuculline (20 μM) completely eliminated both the eIPSPs and APs, confirming that the response is mediated by GABA$_A$Rs (data not shown). In cells that showed occasional AP generation to stimulation of GABAergic inputs, we tested the effects of GABA$_B$R agonist (baclofen) and antagonists (CGP52432 and CGP54626) on the firing probability in response to single-pulse or train stimulation. In four cells where GABA$_A$R-mediated
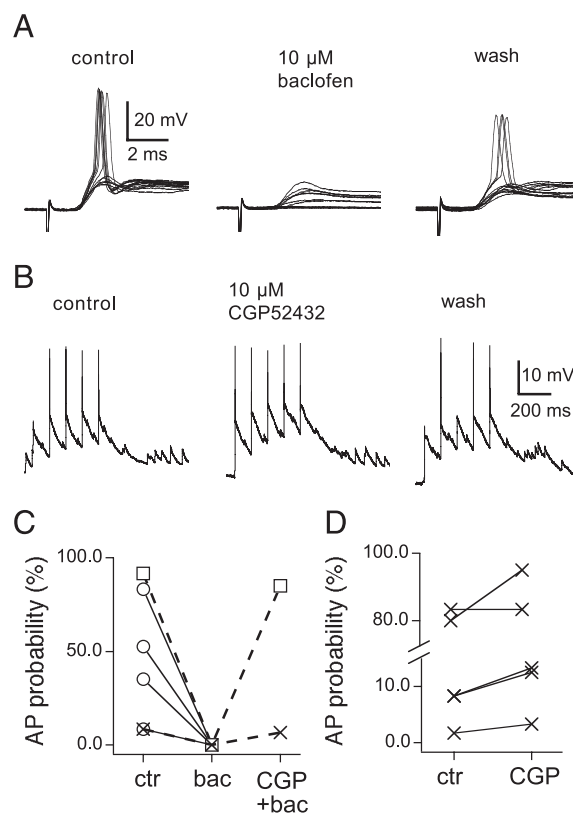

FIG. 8. Effects of baclofen and CGP52432 on GABA-induced action potentials (APs) in NM neurons. *A*: baclofen (10 μM) reduces amplitude of evoked inhibitory postsynaptic potentials (eIPSPs) and eliminates firing in response to activation of depolarizing GABAergic inputs in NM neurons. In this example, 12 superimposed traces in response to single-pulse synaptic stimulation under each condition are shown. After a thorough wash, eIPSP amplitude recovers, and APs resume on the top of some eIPSPs, with unchanged AP parameters except latency (Table 1). Stimulation artifacts truncated for clarity; resting membrane potential (RMP), -68 mV. *B*: CGP52432 (10 μM) slightly increases GABA-induced firing in this neuron without affecting AP parameters (Table 1). Stimulation artifacts truncated for clarity; RMP, -69 mV. *C*: baclofen eliminates APs completely in all 4 cells tested with regular pipettes containing Cl$^-$ of 37 mM (open circles). Baclofen (10 μM) also eliminates APs in 2 cells tested with pipettes containing Cl$^-$ of 55 (crosses) or 60 mM (squares), and the inhibitory effect is blocked by CGP52432 (10 μM). *D*: CGP52432 (10 μM) causes a small but consistent increase in firing probability (6% in average). Cells recorded in current clamp were held at their RMP.

TABLE 1. *Basic properties of GABA-induced APs in NM neurons under control condition, after washout of baclofen (bac wash), and during the application of CGP 52432*

	Control (n = 4)	Bac Wash (n = 4)	t-Test P Value	Control (n = 5)	CGP (n = 5)	t-Test P Value
RMP (mV)	−65.8 ± 3.1	−65.1 ± 2.5	>0.05	−66.5 ± 2.7	−66.8 ± 3.9	>0.05
Latency (ms)	1.17 ± 0.28	1.31 ± 0.30	<0.05*	1.20 ± 0.26	1.21 ± 0.16	>0.05
AP threshold (mV)	−43.9 ± 4.5	−45.9 ± 5.0	>0.05	−46.4 ± 4.9	−45.8 ± 4.2	>0.05
AP height (mV)	25.6 ± 10.5	24.7 ± 10.3	>0.05	23.3 ± 8.4	23.3 ± 9.0	>0.05
AP half-width (ms)	0.30 ± 0.08	0.37 ± 0.12	>0.05	0.35 ± 0.05	0.33 ± 0.10	>0.05

Values are means ± SD. *Significant difference; AP, action potential; NM, nucleus magnocellularis; CGP, CGP52432; RMP, resting membrane potential.

APs were seen (37 mM Cl$^-$ in recording pipettes), baclofen (10 μM for 3 cells and 100 μM for 1 cell) reduced the amplitude of eIPSPs and completely eliminated APs (Fig. 8*C*, open circles). The firing due to activation of GABA$_A$Rs recovered at least partially after washout of baclofen (Fig. 8*A*).

To further confirm that the modulation is mediated by GABA$_B$Rs, we examined the effects of baclofen on GABA-induced APs in the absence and presence of CGP52432. We used a high Cl$^-$ concentration in the internal solution (55 mM in 6 cells and 60 mM in 2 cells, by adding 18 and 23 mM KCl to our regular internal solution, respectively) to increase the probability of obtaining NM neurons that fire GABA-induced APs. This Cl$^-$ concentration is still within the range of physiological intracellular Cl$^-$ concentration in NM neurons measured by perforated-patch techniques (Lu and Trussell 2001). We observed GABA-induced APs in four of eight cells in response to single-pulse stimulation as well as train stimulation (10 Hz; 5 pulses). Two of the four cells that did not generate GABA-induced spikes in response to single-pulse stimulation fired APs in response to the train stimulation. We tested the effects of baclofen and CGP52432 on GABA-induced APs in two cells. Baclofen (10 μM) completely eliminated APs, and this effect was blocked when CGP52432 (10 μM) was present (Fig. 8*C*, squares and crosses).

We measured several basic parameters of GABA-induced APs in NM neurons prior to and after baclofen application, including resting membrane potential (RMP), latency (the time period between the onset of the stimulus and the onset of the response), AP threshold, AP height (difference between the threshold and the peak value), and AP half-width (duration at one-half AP height). No significant differences were detected in these parameters between the APs recorded after washout of baclofen and APs under control condition except latency (Table 1). Baclofen (10 μM) did not change the response latency of eIPSCs (data not shown), so the reason for longer latencies of APs recorded after washout of baclofen is not clear.

We further examined the effects of GABA$_B$R antagonists on the GABA$_A$R-mediated APs. In an additional five cells where GABA$_A$R-mediated APs were seen, the firing probability was 36 ± 42 and 42 ± 44% for control and after bath application of CGP52432 (10 μM), respectively (Fig. 8, *B* and *D*; *P* > 0.05). AP parameters were not altered by CGP52432 application either (Table 1). NM neurons that lacked GABA$_A$R-mediated APs under control condition did not fire in the presence of 10 μM CGP52432 (*n* = 7 cells) or another potent GABA$_B$R antagonist (CGP54626, 10 μM, *n* = 5 cells, data not shown).

The effects of baclofen and CGP52432 on firing rate are not due to a change in excitability of NM neurons because neither baclofen (10 μM) nor CGP52432 (10 μM) altered the excitability of NM neurons. This conclusion is based on experiments in which a series of brief current commands (0.2–1.2 nA with increments of 0.05 nA and 2 ms in duration) were applied to NM neurons before and during drug application (10 repetitions of the current injection protocol under each condition). We plotted AP probability against amplitude of injected currents to measure the threshold current. The threshold current, defined as the current needed to elicit APs at a probability of 50% and used as a measurement of neuronal excitability, was 0.961 ± 0.205 and 0.932 ± 0.086 nA for control and bath application of CGP52432, respectively (*P* > 0.05, *n* = 3 cells), and RMPs under these two conditions were −71.0 ± 2.7 and −70.8 ± 1.9 mV, respectively (*P* > 0.05). The threshold current for control and baclofen-treated neurons was 0.817 ± 0.195 and 0.819 ± 0.295 nA, respectively (*P* > 0.05, *n* = 4 cells), and the RMPs under these two conditions were −69.7 ± 3.2 and −69.0 ± 5.0 mV, respectively (*P* > 0.05).

DISCUSSION

Due to an unusually high intracellular Cl$^-$ concentration in mature NM neurons, depolarizing GABAergic inputs are capable of eliciting APs when the Cl$^-$ channels (GABA$_A$Rs) are activated and Cl$^-$ ions flow out through the postsynaptic membrane of NM neurons (Lu and Trussell 2001; this study). Here we show that activation of GABA$_B$Rs inhibits GABA$_A$R-mediated responses in NM neurons in a dose-dependent manner via a presynaptic mechanism. This modulation may serve as a mechanism preventing NM neurons from firing during activation of the depolarizing inhibitory inputs.

Mechanism for modulation of GABA release by GABA$_B$Rs at NM

GABA$_B$Rs modulate GABA release at NM via a presynaptic mechanism. This conclusion is based on the following observations: *1*) GABA$_B$R agonist baclofen increased the failure rate of eIPSCs in a dose-dependent manner, indicating a presynaptic action of baclofen (Harrison 1990; Ulrich and Huguenard 1996); *2*) baclofen decreased the frequency but not the amplitude of mIPSCs, indicating a modulation of the probability of GABA release (Chen and van den Pol 1998; Jarolimek and Misgeld 1997; Kabashima et al. 1997); and *3*) baclofen at its saturating concentration did not affect postsynaptic currents when postsynaptic GABA$_A$Rs were activated by puff application of a specific GABA$_A$R agonist muscimol, indicating that postsynaptic GABA$_A$Rs are not modulated by GABA$_B$Rs (Chen and van den Pol 1998). Muscimol at high concentrations

has been found to be able to activate $GABA_BRs$ in rat medial nucleus of the trapezoid body (MNTB) neurons with an EC_{50} of 25 μM when bath-applied (Yamauchi et al. 2000). Although we cannot rule out the possibility that brief puff-applied muscimol (500 μM, pressure of 5–10 psi, and duration of 10–50 ms) activated $GABA_BRs$ in NM neurons, and consequently, the observation that baclofen did not modulate muscimol-induced currents was because $GABA_BRs$ were already activated, we want to stress two points. First, when puff-applied, the effective drug concentration is influenced by many factors, including the positive pressure applied, the duration of the application, size and shape of the puff electrodes, distance between the puff electrode tip and the recorded neuron, and the location and abundance of receptors on the neuronal membrane (Marchand and Pearlstein 1995). Hence, the precise drug concentration is hard to determine and is generally smaller than the concentration in the puff pipettes. Kungel and Friauf (1997) reported that a 1,000-fold higher concentration relative to bath application is needed when puff-applying glycine to MNTB neurons to elicit glycine receptor responses. Second, muscimol-induced currents in NM neurons were sensitive (91%) to specific $GABA_AR$ agonist bicuculline. The bicuculline-resistant components (9%) are unlikely due to activation of $GABA_BRs$ because activation of $GABA_BRs$ by baclofen (100 μM) does not elicit any noticeable change in membrane potential of NM neurons (Hyson et al. 1995). Therefore activity of $GABA_BRs$ by muscimol in our case, if any, was likely to be low.

Effects of baclofen on postsynaptic neurons are heterogeneous. Baclofen hyperpolarizes a variety of neurons in the CNS by activating K^+ channels (reviewed in Misgeld et al. 1995), but does not hyperpolarize the membrane potential in many other central neurons (e.g., Misgeld et al. 1989; Newberry and Nicoll 1984; Stevens et al. 1985, 1999). In NM, neither the membrane potential nor the input resistance of NM neurons is changed by puff application of 100 μM baclofen (Hyson et al. 1995) or bath application of 1–100 μM baclofen (this study; data not shown), indicating that postsynaptic $GABA_BRs$ might not be involved in modulation of postsynaptic K^+ channels in NM neurons. This result also indirectly implies that $GABA_BRs$ modulate GABAergic transmission at NM via a presynaptic mechanism.

Lack of endogenous presynaptic $GABA_BR$ activity at NM in slice

$GABA_BRs$ are expressed on presynaptic terminals of many synapses including GABAergic terminals themselves (reviewed in Calver et al. 2002; Misgeld et al. 1995). While agonists of $GABA_BRs$ show dramatic modulatory capability on transmitter release at synapses where $GABA_BRs$ are present, it is unknown under what physiological conditions the receptors are activated (reviewed in Bowery 1993; Misgeld et al. 1995). In theory, endogenous $GABA_BR$ activity should be detectable at the terminals that release GABA and where $GABA_BRs$ function as autoreceptors modulating the transmission. Thus an increase in spontaneous $GABA_AR$-mediated activity in the postsynaptic cells is expected when $GABA_BRs$ are blocked. This has been observed in some cases (e.g., Kabashima et al. 1997; Le Feuvre et al. 1997; Lei and McBain 2002; Stevens et al. 1999) but not in others (reviewed in Misgeld et al. 1995).

We also did not observe endogenous $GABA_BR$ activity in the presynaptic inhibitory terminals in the brain stem slice preparation.

Probability of GABA-induced firing in NM neurons compared with previous studies

Monsivais and Rubel (2001) observed firing of NM neurons in response to synaptic activation of GABAergic inputs only if the LVA K^+ channels were blocked, whereas we observed firing in 32% neurons without blocking the LVA K^+ channels. The discrepancy is likely due to two factors: recording temperature and external Ca^{2+} concentration. While their recordings were done at room temperature (22–23°C), we recorded at higher temperature (34–36°C), which would change the kinetics of eIPSPs. At higher temperature, eIPSPs rise faster, and thus subthreshold inactivation of Na^+ channels is reduced, enhancing the probability of firing. The second factor is that, while they included 2 mM Ca^{2+} in the external solution, we used 3 mM extracellular Ca^{2+}, which would enhance transmitter release (Katz and Miledi 1968; Fig. 2 in this study). Our use of 3 mM Ca^{2+} is based on ion composition analysis done on the chick cerebrospinal fluid (Maki et al. 1990) and previous studies done on the same preparations (e.g., Hackett et al. 1982; Lu and Trussell 2000, 2001).

The percentage of neurons with $GABA_AR$-mediated APs under our condition (13 of 41 neurons; 32%) is smaller than what was reported by Lu and Trussell (2001) (11 of 20 neurons; 55%). This is likely due to the difference in the Cl^- concentrations used in the recording solutions and thus different reversal potentials for Cl^- channels; Lu and Trussell (2001) used 60 and 153 mM Cl^- in their intracellular and extracellular solutions, respectively; ours were 37 and 139 mM, respectively. The calculated reversal potential for Cl^- channels in our hands is –35 mV, about 10 mV more positive than the AP threshold (Monsivais and Rubel 2001), and the calculated reversal potential for the same type channels by Lu and Trussell (2001) is –25 mV, 20 mV more positive than the AP threshold. Therefore in our preparation, the Cl^- driving force (difference between membrane potential and reversal potential) is lower for the $GABA_AR$-mediated depolarization (assuming the same resting membrane potentials for NM neurons), compared with Lu and Trussell (2001). This is confirmed by our observation that when we increased Cl^- concentration in the internal solution to 55 (n = 6 cells) or 60 mM (n = 2 cells), GABA-induced APs in response to single-pulse stimulation were seen in four of eight NM neurons (50%, data not shown).

Functional significance

Avian auditory nerve axons bifurcate as they enter the brain stem to innervate NM and nucleus angularis (NA). Phase-locking NM neurons provide the sole excitatory input bilaterally to nucleus laminaris (NL). SON neurons are driven primarily by inputs from NA as well as NL, and in turn, feed back intensity-dependent GABAergic inhibition to NA, NL, and NM (Burger et al. 2004). Thus NM receives input from only a few sources, large endbulb type excitatory inputs from eighth nerve fibers and GABAergic input arising primarily from SON (Burger et al. 2004; Lachica et al. 1994; Parks and Rubel 1975;

Rubel and Parks 1975; Yang et al. 1999). Despite the apparent simplicity conferred by the small number of inputs to NM, a growing body of evidence suggests a rich intercellular signaling milieu, where several mechanisms converge to enhance temporal processing for sound localization. The presence of presynaptic GABA$_B$Rs on the inhibitory terminals adds to this complexity and contributes to the well-characterized function of these neurons. This discovery follows several previous studies that reveal various mechanisms by which the GABAergic input to NM influences its role in temporal processing.

First, GABAergic input to NM directly controls glutamate release at the excitatory terminals. Presynaptic GABA$_B$Rs restrict eighth nerve vesicle release such that the pool of available vesicles is retained during high-frequency firing (Brenowitz et al. 1998; Otis and Trussell 1996). This functions to preserve the efficacy of the synapse over a range of input rates. In a subsequent study, Brenowitz and Trussell (2001) showed that this control of glutamate release improves reliability of the eighth nerve signaling by preventing glutamate receptor desensitization at NM synapses.

Second, Monsivais and colleagues, in this laboratory (Monsivais and Rubel 2001; Monsivais et al. 2000), showed the efficacy of the unusual depolarizing property of GABAergic inputs in suppressing responses to the large excitatory inputs from auditory nerve fibers by activating a large LVA K$^+$ conductance and simultaneously inactivating voltage-gated Na$^+$ channels. Thus the depolarizing influence of GABA postsynaptically in NM preserves and even enhances the remarkable temporal integration properties of the NM cell membrane when the SON input is activated.

Finally, a complimentary series of studies by Lu and Trussell (2000, 2001) showed that the GABAergic terminals in NM prominently display Ca^{2+}-dependent asynchronous release during high stimulation rates, resulting in long depolarized plateaus in NM via postsynaptic GABA$_A$Rs. Paradoxically, these depolarizing GABAergic inputs were shown to occasionally evoke spikes in NM. These spikes, should they occur in vivo, would almost certainly be temporally uncorrelated with the stimulus and reduce the ability of NM to provide phase-locked input to NL.

Here we show an additional site of GABA-dependent signaling that is sufficient to prevent GABA-evoked spiking. Firing of NM neurons in response to stimulation of GABAergic inputs was completely eliminated during application of GABA$_B$R agonist baclofen, indicating that modulation of GABA release by presynaptic GABA$_B$Rs is sufficient to suppress GABA-induced firing in NM neurons that may interfere with the critical temporal fidelity of NM output.

Within the relatively simple synaptic architecture of this "relay" nucleus, this and previous studies reveal a rich interplay between a highly efficacious excitatory input and an unusual depolarizing and potent inhibition. These inputs converge and interact through ionotropic and metabotropic receptors on both pre- and postsynaptic elements. Each input is thus highly regulated to enhance the temporal coding properties of NM output. This study contributes to this view by revealing a previously unknown mechanism by which the crucial but potentially disruptive GABA-induced depolarization is regulated.

REFERENCES

Allen C and Stevens CF. An evaluation of causes for unreliability of synaptic transmission. *Proc Natl Acad Sci USA* 91: 10380–10383, 1994.

Bowery NG. GABA$_B$ receptor pharmacology. *Ann Rev Pharmac Toxicol* 33: 109–147, 1993.

Brenowitz S, David J, and Trussell LO. Enhancement of synaptic efficacy by presynaptic GABA$_b$ receptors. *Neuron* 20: 135–141, 1998.

Brenowitz S and Trussell LO. Minimizing synaptic depression by control of release probability. *J Neurosci* 21: 1857–1867, 2001.

Burger RM, Cramer KS, Pfeiffer JD, and Rubel EW. The avian superior olivary nucleus provides divergent inhibitory input to parallel auditory pathways. *J Comp Neurol* 481: 6–18, 2005.

Calver AR, Davies CH, and Pangalos M. GABA$_B$ receptors: from monogamy to promiscuity. *Neurosignals* 11: 299–314, 2002.

Canepari M and Cherubini E. Dynamics of excitatory transmitter release: analysis of synaptic responses in CA3 hippocampal neurons after repetitive stimulation of afferent fibers. *J Neurophysiol* 79: 1977–1988, 1998.

Chen G and van den Pol AN. Presynaptic GABA$_B$ autoreceptor modulation of P/Q-type calcium channels and GABA release in rat suprachiasmatic nucleus neurons. *J Neurosci* 18: 1913–1922, 1998.

Debanne D, Guerineau NC, Gahwiler BH, and Thompson SM. Paired-pulse facilitation and depression at unitary synapses in rat hippocampus: quantal fluctuation affects subsequent release. *J Physiol* 491: 163–176, 1996.

Hackett JT, Jackson H, and Rubel EW. Synaptic excitation of the second and third order auditory neurons in the avian brain stem. *Neuroscience* 7: 1455–1469, 1982.

Harrison NL. On the presynaptic action of baclofen at inhibitory synapses between cultured rat hippocampal neurones. *J Physiol* 422: 433–446, 1990.

Hyson RL, Reyes AD, and Rubel EW. A depolarizing inhibitory response to GABA in brainstem auditory neurons of the chick. *Brain Res* 677: 117–126, 1995.

Jarolimek W and Misgeld U. GABA$_B$ receptor-mediated inhibition of tetrodotoxin-resistant GABA release in rodent hippocampal CA1 pyramidal cells. *J Neurosci* 17: 1025–1032, 1997.

Jiang L, Sun S, Nedergaard M, and Kang J. Paired-pulse modulation at individual GABAergic synapse in rat hippocampus. *J Physiol* 523: 425–439, 2000.

Kabashima N, Shibuya I, Ibrahim N, Ueta Y, and Yamashita H. Inhibition of spontaneous EPSCs and IPSCs by presynaptic GABA$_B$ receptors on rat supraoptic magnocellular neurons. *J Physiol* 504: 113–126, 1997.

Katz B and Miledi R. The role of calcium in neuromuscular facilitation. *J Physiol* 195: 481–492, 1968.

Kungel M and Friauf E. Physiology and pharmacology of native glycine receptors in developing rat auditory brainstem neurons. *Brain Res Dev Brain Res* 102: 157–165, 1997.

Lachica EA, Rübsamen R, and Rubel EW. GABAergic terminals in nucleus magnocellularis and laminaris originate from the superior olivary nucleus. *J Comp Neurol* 348: 403–418, 1994.

Le Feuvre Y, Fricker D, and Leresche N. GABA$_A$ receptor-mediated IPSCs in rat thalamic sensory nuclei: patterns of discharge and tonic modulation by GABA$_B$ autoreceptors. *J Physiol* 502: 91–104, 1997.

Lei S and McBain CJ. GABA$_B$ receptor modulation of excitatory and inhibitory synaptic transmission onto rat CA3 hippocampal interneurons. *J Physiol* 546: 439–453, 2002.

Lu T and Trussell LO. Inhibitory transmission mediated by asynchronous transmitter release. *Neuron* 26: 683–694, 2000.

Lu T and Trussell LO. Mixed excitatory and inhibitory GABA-mediated transmission in chick cochlear nucleus. *J Physiol* 535: 125–131, 2001.

Lu Y, Burger RM, and Rubel EW. GABA$_b$ receptor activation modulates GABA$_a$ receptor-mediated inhibition in chicken nucleus magnocellularis neurons. *Assoc Res Otolaryngol Midwinter Mtg Abstr* 27: 316–317, 2004.

Maki AA, Beck MM, Gleaves EW, DeShazer JA, and Eskridge KM. CSF ion composition and manipulation during thermoregulation in an avian species, Gallus domesticus. *Comp Biochem Physiol A* 96: 135–140, 1990.

Marchand AR and Pearlstein E. A simple dual pressure-ejection system and calibration method for brief local applications of drugs and modified salines. *J Neurosci Methods* 60: 99–105, 1995.

Misgeld U, Bijak M, and Jarolimek W. A physiological role for GABA$_B$ receptors and the effects of baclofen in the mammalian central nervous system. *Prog Neurobiol* 46: 423–462, 1995.

Misgeld U, Muller W, and Brunner H. Effects of (-)baclofen on inhibitory neurons in the guinea pig hippocampal slice. *Pfluegers* 414: 139–144, 1989.

Monsivais P and Rubel EW. Accomodation enhances depolarizing inhibition in central neurons. *J Neurosci* 21: 7823–7830, 2001.

Monsivais P, Yang L, and Rubel EW. GABAergic inhibition in nucleus magnocellularis: implications for phase locking in the avian auditory brainstem. *J Neurosci* 20: 2954–2963, 2000.

Newberry NR and Nicoll RA. Direct hyperpolarizing action of baclofen on hippocampal pyramidal cells. *Nature* 308: 450–452, 1984.

Oertel D. The role of timing in the brain stem auditory nuclei of vertebrates. *Annu Rev Physiol* 61: 497–519, 1999.

Otis TS and Trussell LO. Inhibition of transmitter release shortens the duration of the excitatory synaptic current at a calyceal synapse. *J Neurophsyiol* 76: 3584–3588, 1996.

Parks TN and Rubel EW. Organization and development of brain stem auditory nuclei of the chicken: organization of projections from n. magnocellularis to n. laminaris. *J Comp Neurol* 164: 435–448, 1975.

Parks TN and Rubel EW. Organization and development of the brain stem auditory nuclei of the chicken: primary afferent projections. *J Comp Neurol* 180: 439–448, 1978.

Pena JL, Viete S, Albeck Y, and Konishi M. Tolerance to sound intensity of binaural coincidence detection in the nucleus laminaris of the owl. *J Neurosci* 16: 7046–7054, 1996.

Pfeiffer J, Burger RM, and Rubel EW. Development of GABA$_B$ receptor immunoreactivity in the avian auditory nuclei. *Assoc Res Otolaryngol Midwinter Mtg Abstr* 26: 155, 2003.

Reyes AD, Rubel EW, and Spain WJ. Membrane properties underlying the firing of neurons in the avian cochlear nucleus. *J Neurosci* 14: 5352–5364, 1994.

Rubel EW and Parks TN. Organization and development of brain stem auditory nuclei of the chicken: tonotopic organization of n. magnocellularis and n. laminaris. *J Comp Neurol* 164: 411–433, 1975.

Stevens DR, Gallagher JP, and Shinnick Gallagher P. Further studies on the action of baclofen on neurons of the dorsolateral septal nucleus of the rat in vitro. *Brain Res* 358: 360–363, 1985.

Stevens DR, Kuramasu A, and Haas HL. GABA$_B$-receptor-mediated control of GABAergic inhibition in rat histaminergic neurons in vitro. *Eur J Neurosci* 11: 1148–1154, 1999.

Trussell LO. Synaptic mechanisms for coding timing in auditory neurons. *Annu Rev Physiol* 61: 477–496, 1999.

Ulrich D and Huguenard JR. Gamma-aminobutyric acid type B receptor-dependent burst-firing in thalamic neurons: a dynamic clamp study. *Proc Natl Acad Sci USA* 93: 13245–13249, 1996.

Yamauchi T, Hori T, and Takahashi T. Presynaptic inhibition by muscimol through GABA$_B$ receptors. *Eur J Neurosci* 12: 3433–3436, 2000.

Yang L, Monsivais P, and Rubel EW. The superior olivary nucleus and its influence on nucleus laminaris: a source of inhibitory feedback for coincidence detection in the avian auditory brainstem. *J Neurosci* 19: 2313–2325, 1999.